Targeting Insulin-like Growth Factor I with 10-23 DNAzymes: 2 '-O-Methyl Modifications in the Catalytic Core Enhance mRNA Cleavage

ARTICLE *in* BIOCHEMISTRY · MARCH 2012

Impact Factor: 3.02 · DOI: 10.1021/bi201532q · Source: PubMed

5 AUTHORS, INCLUDING:

Mariya I Meschaninova
Russian Academy of Sciences
22 PUBLICATIONS **202** CITATIONS

BIOCHEMISTRY
including biophysical chemistry & molecular biology

Article

pubs.acs.org/biochemistry

Targeting Insulin-like Growth Factor I with 10−23 DNAzymes: 2′-O-Methyl Modifications in the Catalytic Core Enhance mRNA Cleavage

Alesya A. Fokina,[†,‡,§,∥] Mariya I. Meschaninova,[§] Tiphanie Durfort,[†,‡,∥] Alya G. Venyaminova,[§] and Jean-Christophe François*[,†,‡,∥,⊥]

[†]INSERM, U565, Acides nucléiques: dynamique, ciblage et fonctions biologiques, 75005 Paris, France

[‡]MNHN, USM503, Département de "Régulations, développement et diversité moléculaire", Laboratoire des Régulations et Dynamique des génomes, Paris, France

[§]Laboratory of RNA Chemistry, Institute of Chemical Biology and Fundamental Medicine, Novosibirsk, Siberian Division of Russian Academy of Sciences (SB-RAS), 630090 Novosibirsk, Russia

[∥]CNRS, UMR7196, Acides nucléiques: dynamique, ciblage et fonctions biologiques, 75005 Paris, France

Supporting Information

ABSTRACT: Insulin-like growth factor I (IGF-I) and its cognate receptor (IGF-1R) contribute to normal cell function and to tumorigenesis. The role of IGF-I signaling in tumor growth has been demonstrated in vivo using nucleic acid-based strategies. Here, we designed the first 10−23 DNAzymes directed against IGF-I mRNA. Unlike antisense approaches and RNA interference that require protein catalysis, DNAzymes catalyze protein-free RNA cleavage. We identified target sequences and measured catalytic properties of differently designed DNAzymes on short synthetic RNA targets and on in vitro transcribed IGF-I mRNA. The most efficient cleavers were then transfected into cells, and their inhibitory effect was analyzed using reporter gene assays. We found that increasing the size of DNAzyme flanking sequences and modifications of the termini with 2′-O-methyl residues improved cleavage rates of target RNAs. Modification of the catalytic loop with six 2′-O-methyl ribonucleotides at nonessential positions increased or decreased catalytic efficiency depending on the mRNA target site. In cells, DNAzymes with 2′-O-methyl-modified catalytic cores and flanking sequences were able to inhibit reporter gene activity because of specific recognition and cleavage of IGF-I mRNA sequences. Mutant DNAzymes with inactive catalytic cores were unable to block reporter gene expression, demonstrating that the RNA cleaving ability of 10−23 DNAzymes contributed to inhibitory mechanisms. Our results show that nuclease-resistant 2′-O-methyl-modified DNAzymes with high catalytic efficiencies are useful for inhibiting IGF-I gene function in cells.

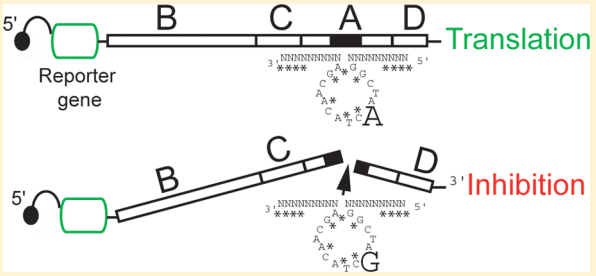

Nucleic acid-based approaches to modulating gene expression are useful for understanding gene function and for therapeutic purposes.[1] Widely used in cells and in vivo are strategies based on short synthetic nucleic acids that block gene expression specifically during translation. Two main mechanisms are involved in translation inhibition. Either the oligonucleotides interfere physically with target RNA without cleaving it, or they induce cleavage of their target at specific sites triggering RNA degradation. Physical blockade of ribosome scanning during translation or modulation of RNA splicing can be achieved using single-stranded oligonucleotides chemically modified to compete with spliceosome machinery or to act as steric blockers.[2] In most cases, binding of short complementary nucleic acids to the mRNA target induces its specific degradation, because of the recruitment of cellular proteins. In the antisense strategy, the mRNA binding of the oligodeoxynucleotide recruits ribonuclease H (RNase H), which cleaves the RNA moiety of RNA−DNA hybrids.[3] In the RNA interference approach, double-stranded short interfering RNAs (siRNAs) destroy specifically a complementary mRNA with the help of a specialized intracellular protein complex, the RNA-induced silencing complex (RISC).[3]

In addition to these two strategies, some nucleic acids, first termed ribozymes, are able to induce RNA cleavage in a manner independent of protein catalysis when bound to complementary sequences.[4] Among site-specific RNA-cleaving nucleic acid molecules, catalytic DNAs (DNAzymes or deoxyribozymes) have received much attention. These small DNAs that induce site-specific cleavage of target RNA were developed by an in vitro selection procedure.[5] The most commonly used catalytic DNA, the 10−23 DNAzyme, consists of a 15-nucleotide catalytic core flanked by two substrate recognition domains and can cleave complementary RNA targets with high efficiency under simulated physiological conditions.[6] Cleavage occurs in a sequence-specific manner between an unpaired purine (R) and a paired pyrimidine (Y). The 10−23

Received: October 3, 2011
Revised: February 17, 2012
Published: February 21, 2012

DNAzymes cleave a broad range of RNA targets in vitro and in vivo.[7,8]

The ability of 10−23 DNAzymes to interfere with gene expression is highly dependent on catalytic activity, stability in biological media, and efficiency of intracellular delivery. Their cleaving activity is sensitive to targeted RY dinucleotides: DNAzymes targeting AU or GU are more efficient than those targeting GC or AC.[9] RNA cleavage rates increase with the introduction of intercalators or substitution of deoxyguanine with deoxyinosine at the junctions of the catalytic loop and hybridizing domain.[9,10] The 10−23 DNAzyme activity in cells also was enhanced when the nuclease resistance and ability to hybridize are improved, especially when targeting structured mRNA. Modification of flanking arm extremities by a few phosphorothioates,[11] 2′-O-methyl nucleotides,[12−15] N3′−P5′ phosphoramidates,[16] or locked nucleoside analogues[17−19] confers nuclease resistance and increases RNA complex stability.

Insulin-like growth factor I (IGF-I) and its cognate receptor (IGF-1R) play critical roles in the growth, development, and homeostasis in vertebrate organisms. They contribute to tumorigenesis and are validated targets for nucleic acid-based inactivation. Inhibition of IGF-I or IGF-1R gene expression by antisense RNA, antisense oligonucleotides, or triplex-forming RNA suppresses oncogenic transformation and leads to regression of experimental tumors concomitantly triggering an antitumoral immune response in animal models.[20−22] Other approaches such as triplex-forming oligonucleotides, antisense steric blockers, short interfering RNAs, and ribozymes have been successfully applied to inhibit IGF functions.[23−29]

Here, we developed 10−23 DNAzymes to block expression from IGF-I mRNA in tumor cells, with the ultimate goal of inhibiting tumorigenesis. We designed and studied several 10−23 DNAzymes with 2′-O-methyl ribonucleotides in the flanking arms and catalytic core. They efficiently cleaved rat IGF-I mRNA in vitro, and we validated this activity in living cells using a reporter assay.

EXPERIMENTAL PROCEDURES

Oligonucleotide Synthesis and Purification. Short RNA substrates and DNAzymes were made with an automatic ASM-800 DNA/RNA synthesizer (Biosset, Novosibirsk, Russia) using deoxy-, ribo-, and 2′-O-methyl ribo-β-cyanoethyl phosphoramidites (Glen Research, Sterling, VA). Oligonucleotides with 3′-terminal thymidine linked by a 3′−3′ phosphodiester bond were synthesized using the solid support with attached 3′-O-dimethoxytritylthymidine. Deprotected oligonucleotides were purified by denaturing 20% PAGE with 8 M urea. After UV detection, products were eluted from gels with 0.3 M $LiClO_4$ desalted on Sep-Pac C18 (Millipore, Bedford, MA) and precipitated as lithium salts. The absorbance at 260 nm was determined using a NanoDrop spectrophotometer (Thermo Scientific, Wilmington, DE). Concentrations were calculated with molar extinction coefficients provided by OligoAnalyzer version 3.1 (Integrated DNA Technologies, Inc., Coralville, IA).

Plasmids. pGEM-T7-rIGF-I contains the rat IGF-I cDNA flanked by T7 and SP6 promoters. A plasmid encoding a partial sequence of rat preproIGF-I cDNA[30] was used as a polymerase chain reaction (PCR) template with two long primers to introduce the first 16 N-terminal amino acids of rat IGF-I and the XbaI restriction enzyme site. An amplicon containing the full-length rat IGF-I mature peptide sequence was subcloned into the XbaI-linearized pGEM9Z plasmid (Promega, Madison, WI) to give pGEM-T7-rIGF-I. Rat IGF-I cDNA fused to *Renilla* luciferase was obtained after amplification of a 1833-nucleotide PCR fragment from I.M.A.G.E. clone 7300903 (http://www.geneservice.co.uk) using two primers containing PvuI and NotI sites and SP6/T7 promoter binding sequences (5′-ATCGATCGATATTTAGGTGACACTATAGAA-3′ and 5′-TATAGCGGCCGCTAATACGACTCACTATAGG-3′). After PvuI and NotI digestion, the rat IGF-I containing a PCR fragment was subcloned into psiCHECK2, opened at SgfI and NotI sites immediately downstream of the synthetic humanized *Renilla* luciferase (hRluc) coding sequence (Promega). The synthetic firefly luciferase gene (hluc+) was then deleted by NarI digestion followed by ligation to give psick-rIGF1(1833)-ΔFluc. All plasmid sequences were confirmed by sequencing both strands of DNA inserts (Cogenics, Grenoble, France). pGL2-CMV is a plasmid with firefly luciferase (F-luc) under control of the human cytomegalovirus promoter.[31]

Preparation of RNA Substrates. Synthetic RNA substrates were radiolabeled at the 5′ end using T4 polynucleotide kinase (10 units, Sibenzyme, Novosibirsk, Russia). The substrate, 3.7 MBq of [γ-^{32}P]ATP (148 PBq/mol; Biosan, Novosibirsk, Russia), and 10% DMSO were incubated in Tris buffer [50 mM Tris-HCl (pH 7.6), 10 mM $MgCl_2$, and 5 mM dithiothreitol] for 2 h at 37 °C. Following this incubation, 5 units of kinase was added, and the samples were incubated for 1 h; an additional 5 units of kinase and 10 mM ATP were added, and the sample was incubated for 1 h. The ^{32}P-labeled short RNAs were purified by 20% denaturing PAGE. Fragments were recovered from the gel and concentrations determined as described above.

The long IGF-I RNA target was obtained from in vitro transcription of pGEM-T7-rIGF-I. This plasmid was first linearized using HindIII to allow in vitro runoff transcription using the RiboMAX large-scale production system with T7 RNA polymerase (Promega). The 360-nucleotide transcript corresponding to mature rat IGF-I mRNA was purified on Micro Bio-Spin 30 columns in RNase-free Tris buffer (Bio-Rad, Hercules, CA). The transcript was dephosphorylated before labeling. The RNA transcript (1 μg/μL) was heated to 80 °C for 5 min and immediately added to the reaction mix [50 mM Tris-HCl (pH 8.5), 0.1 mM Na_2EDTA, and 2% formamide] containing 2 units of calf intestine alkaline phosphatase (Roche Diagnostics, Meylan, France). Dephosphorylation lasted for 1 h at 50 °C, followed by a second addition of phosphatase (1 unit) and incubation for 30 min. After extraction with phenol and chloroform and precipitation with ethanol, dephosphorylated RNA was dissolved in RNase-free water. The 5′ ^{32}P labeling of the RNA transcript was performed as described for the synthetic short RNA except that 18.5 MBq of [γ-^{32}P]ATP, 20 units of T4 polynucleotide kinase, and 15% DMSO were added to the reaction mixture and no additional incubation with 10 mM ATP was performed. For cleavage product size analysis, the RNA transcript was labeled during in vitro transcription using 370 kBq of [α-^{32}P]UTP (14.8 GBq/mol). Labeled RNA was purified by 8% denaturing PAGE, eluted overnight by extraction with 300 μL of 0.3 M sodium acetate (pH 5.0) with 0.1% SDS, and precipitated with ethanol.

In Vitro Cleavage of RNA Substrates by DNAzymes. Cleavage assays with short RNA substrates were performed under single- or multiple-turnover conditions with DNAzymes incubated in 50 mM Tris-HCl buffer (pH 7.5) and 10 mM $MgCl_2$. For single-turnover assays, synthetic RNA target and

DNAzymes (in excess) were mixed in reaction buffer, heated to 95 °C for 2 min, and incubated at 37 °C for 10 min. The reactions were initiated by addition of $MgCl_2$ to a final concentration of 10 mM, and the mixtures were incubated at 37 °C. For multiple-turnover assays, DNAzyme and substrate (in excess) were denatured separately in reaction buffer at 95 °C for 1 min and then cooled to 37 °C for 10 min. $MgCl_2$ was added to both solutions, and each solution was incubated at 37 °C for 15 min before the cleavage reaction was initiated by combining substrate and DNAzyme solutions. For IGF-I transcript cleavage assays, DNAzyme and RNA transcript (100 nM) were incubated separately in reaction buffer [50 mM Tris-HCl (pH 7.5), 200 mM KCl, and 10 mM $MgCl_2$] for 5 min at 37 °C, before cleavage reactions were started by combining both solutions. For kinetic assays, 3 μL aliquots were taken from the reaction mixture at the appropriate time points; reactions were quenched by addition of 6 μL of stop buffer (8 M urea, 90 mM Tris-borate, 50 mM EDTA, 0.05% bromophenol blue, and xylene cyanol FF), and mixtures were loaded onto 20 or 8% denaturing gels for short RNA or IGF-I transcript cleavage assays, respectively. Images from dried gels were taken with a Molecular Imager FX (Bio-Rad) and quantified using Gel-Pro Analyzer version 3.1 (Media Cybernetics, Silver Spring, MD). Fragment size was estimated from the log relation of the expected product length to migration on denaturing PAGE.

Determination of Catalytic Parameters of DNAzymes. To determine the observed rate of cleavage (k_{obs}) on both short and long RNA targets, data from single-turnover assays were fit using Origin version 7.0 (Origin Lab, Northampton, MA) with the single-exponential decay function $P(t) = P\infty \times \exp(-k_{obs}t)$, where $P(t)$ is the extent of cleavage at time t (minutes) and $P\infty$ is the limiting extent of cleavage. For the multiple-turnover assay with a short RNA substrate, a linear regression model [$P(t) = v_0t$, where v_0 is the initial rate of cleavage] was fit to the first five data points, corresponding to the initial 10% of the reaction. DNAzyme kinetic parameters K_m and k_{cat} were determined under single-turnover conditions for both RNA targets. DNAzyme and substrate concentrations are indicated in figure legends. Gels were analyzed by nonlinear curve fitting to obtain the cleavage rate. K_m and k_{cat} were obtained using data from five or six DNAzyme concentrations using Origin version 7.0 (Origin Lab) by a nonlinear regression fit of Michaelis–Menten curves {$k_{obs} = k_{cat}/[1 + K_m/\mathrm{Co(Dz)}]$ where Co(Dz) is the DNAzyme concentration}.

Determination of DNAzyme Binding Affinities. The 5′-end-labeled noncleavable short RNA target NC-FRS was incubated with increasing concentrations of modified DNAzymes at 37 °C for 1 h in 50 mM Tris-HCl buffer (pH 7.5) containing 150 mM NaCl and 0.5 mM $MgCl_2$. Analysis of complexes was performed at 37 °C by electrophoresis on a nondenaturing 10% polyacrylamide gel in Hepes-Mg buffer [50 mM Hepes (pH 7.5) and 0.5 mM $MgCl_2$]. The concentration at which 50% of the duplex was formed (C_{50}) was reported (mean of two independent experiments).

Cell Culture, DNAzyme, and Plasmid Transfection. The LFCL2A rat hepatocarcinoma cell line used for transfection of DNAzymes was maintained in minimal essential medium (Invitrogen, Cergy-Pontoise, France) containing 2 mM glutamine and 10% (v/v) fetal calf serum, which was heat inactivated for 30 min at 60 °C.[21] The absence of mycoplasma was regularly ensured using PCR (VenorGeM, Biovalley, Marne-la-Vallée, France). Cotransfections of plasmids and DNAzymes were performed with Lipofectamine 2000 (Invitrogen).

Reporter Gene Assays. Luciferase activities from *Photinus pyralis* (F-luc) and *Renilla reniformis* (R-luc) were measured after cell harvesting using the dual-luciferase assay kit (Promega). After lysis in passive lysis buffer, luminescence was measured sequentially for both luciferases in the same well using a microplate luminometer (Victor2, Wallac, Wellesley, MA) with one injector filled with *P. pyralis* luciferase substrates and the second injector filled with *R. reniformis* substrate with a quencher of the *P. pyralis* luciferase. Relative luciferase activity was calculated by dividing *R. reniformis* R-luc activity by *P. pyralis* F-luc activity, allowing normalization of transfection efficiency. All transfection assays were performed at least twice, and each consisted of four independent transfections.

Statistical Analyses. The observed cleavage rate and initial velocity were determined two or three times from DNAzyme cleavage assays performed with 5′-radiolabeled RNA targets. The indicated error in the initial velocity represents an estimated deviation obtained after the fitting procedure with the equations given above, and those of kinetic parameters represent estimated deviations obtained by a least-squares fitting procedure with the Michaelis–Menten equation. All transfection data are presented as means ± the standard error of the mean (SEM) and were analyzed using ANOVA from GraphPad Prism 5 followed by the Dunnett post hoc test. P values of <0.05 were considered significant.

RESULTS

Identification of Target Sequences on IGF-I mRNA. IGF-I mRNA has been targeted with antisense oligonucleotides and short interfering RNAs in cell culture.[32−34] Here, we designed DNAzymes against IGF-I mRNA following a set of rules. We aligned rodent IGF-I mRNA sequences to determine conserved regions. We identified two targets, which are subsequently termed target sites for GAEL and FRS oligomers (Figure 1A). These sites are in the coding region of rat IGF-I in accessible regions according to a minimal free energy prediction of the mRNA secondary structure (Figure S1 of the Supporting Information). Alignments with rat IGF-2 and insulin mRNAs, both highly homologous to IGF-I, revealed that targeting these sites would ensure high selectivity and specificity for IGF-I mRNA (Figure S2 of the Supporting Information). We then designed 10−23 DNAzymes for cleaving GC or GU dinucleotides in these two sites according to the preferred cleavage site rule for efficient DNAzymes.[9] A series of DNAzymes differing in the length of flanking sequences from 8 to 10 nucleotides were synthesized (Table S1 of the Supporting Information). A series of DNAzymes were targeted to GC (GAEL and FRS_{GC}) and a series to the GU dinucleotide (FRS_{GU}) (Figure 1B).

Selection of the Flanking Sequences of DNAzymes. DNAzyme series complementary to GAEL and FRS sites were screened for efficient cleavage of short RNA substrates. To protect them from nucleases, all DNAzymes were modified by an "inverted" 3′ end thymidine (Figure 1B).[35] The flanking sequences of 10−23 DNAzymes, which contribute to DNAzyme–RNA substrate duplex stability, play an essential role in the catalytic activity. To design substrate recognition domains with optimal stability, each flanking sequence should have a predicted ΔG°_{37} of −8 to −10 kcal/mol.[36] Increasing the length of the DNAzyme flanking sequence (from 8 to 9 or

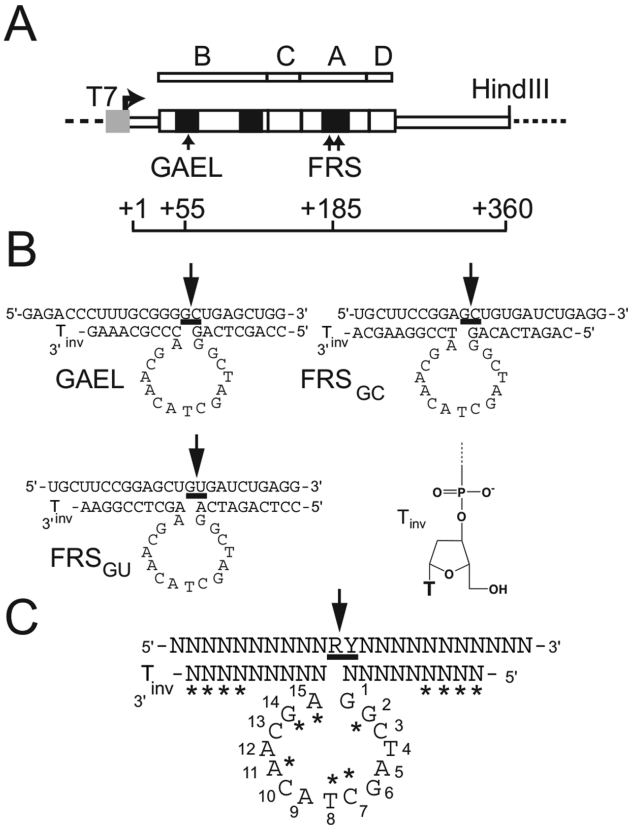

Figure 1. DNAzymes targeting IGF-I mRNA. (A) Schematic representation of GAEL and FRS target sites on pGEM-T7-rIGF-I. T7 indicates the T7 RNA polymerase promoter. B, C, A, and D domains of mature IGF-I protein are shown at the top. The position of target sites (arrows) is also indicated as nucleotides from the transcription start. (B) Sequences of 10–23 DNAzymes that are all 3′-modified with an inverted 3′–3′ thymidine (Tinv). Cleavage occurred at the positions marked with arrows on short complementary oligoribonucleotides used for catalytic activity studies: 25ST-GAEL and 24ST-FRS for GAEL and FRS DNAzymes, respectively. Only DNAzymes with the longest hybridizing sequences are shown. (C) Schematic representation of 2′-O-methylnucleotide-containing DNAzymes. Positions of modified nucleotides in the flanking sequences and catalytic core are labeled with asterisks.

10 nucleotides) improved the efficiency of cleavage of the short substrates (Table 1).

To improve the cleavage efficiency of DNAzymes targeted to GC dinucleotides, we replaced the deoxyguanosine 5′ of the catalytic core with deoxyinosine (Table S2 of the Supporting Information). Wobble pairing of inosine to cytosine was previously shown to increase the cleavage rate.[9] Indeed, this modification improved the cleavage of synthetic short RNAs in all our DNAzymes. The largest enhancement was 8-fold, achieved in DNAzymes targeted to GAEL.

2′-O-Methyl Ribonucleotide Modifications in the Binding Arms and Catalytic Domain. To increase the affinity for the RNA target and improve nuclease resistance, we replaced some deoxynucleotides with 2′-O-methyl analogues at the end of the substrate binding domains or in the catalytic loop (Figure 1C).[12,14] Cleavage activities were evaluated using short synthetic RNA substrates (Table 1). The insertion of 2′-O-methyl ribonucleotides into the DNAzyme substrate binding domains increased the RNA cleavage efficiency under single-turnover conditions, particularly with GAEL9/9I and

Table 1. Catalytic Activities of DNAzymes[a]

DNAzyme	k_{cleav} (min^{-1})[b]	k_{obs} (min^{-1})[c]	v_o (nM min^{-1})[d]
GAEL9/9	–	0.064 ± 0.009	0.21 ± 0.01
GAEL9/9I	0.48 ± 0.06	0.310 ± 0.050	1.23 ± 0.02
GAEL9^m/9^mI	0.5 ± 0.1	0.400 ± 0.030	0.82 ± 0.02
GAEL9^m/9^mIL^m	0.22 ± 0.04	0.230 ± 0.010	0.5 ± 0.01
FRS_{GC}9/9	–	0.015 ± 0.002	0.081 ± 0.001
$FRS_{GC}9^m$/9^m	0.033 ± 0.004	0.026 ± 0.004	0.068 ± 0.002
$FRS_{GC}9^m$/9^mL^m	0.030 ± 0.003	0.031 ± 0.004	0.084 ± 0.002
FRS_{GC}9/10	–	0.024 ± 0.004	0.09 ± 0.002
$FRS_{GC}9^m$/10^m	0.035 ± 0.004	0.031 ± 0.007	0.075 ± 0.001
$FRS_{GC}9^m$/10^mL^m	0.033 ± 0.003	0.032 ± 0.005	0.062 ± 0.001
FRS_{GC}10/10	–	0.026 ± 0.005	0.071 ± 0.001
FRS_{GU}9/8	–	0.18 ± 0.01	0.30 ± 0.01
$FRS_{GU}9^m$/8^m	6.8 ± 0.5	1.5 ± 0.2	1.25 ± 0.02
$FRS_{GU}9^m$/8^mL^m	4.1 ± 0.3	1.2 ± 0.1	1.45 ± 0.02
FRS_{GU}9/9	–	0.70 ± 0.07	1.27 ± 0.06
$FRS_{GU}9^m$/9^m	8.3 ± 0.7	2.4 ± 0.2	2.10 ± 0.04
$FRS_{GU}9^m$/9^mL^m	4.0 ± 0.3	1.7 ± 0.1	0.91 ± 0.02
FRS_{GU}10/10	–	2.0 ± 0.2	2.2 ± 0.2

[a]All parameters were determined for cleavage of IGF-I short synthetic RNA targets by DNAzymes in a buffer containing 50 mM Tris-HCl (pH 7.5) and 10 mM $MgCl_2$ at 37 °C. The DNAzyme name indicates the target site, the type of targeted dinucleotide, and the length of the 3′ and 5′ arms flanking the catalytic loop. L represents the sequence of the DNAzyme catalytic core (5′-GGCTAGCTACAACG-3′); I stands for deoxyinosine. A superscript m indicates 2′-O-methyl modifications (positions denoted with asterisks on the DNAzyme structure in Figure 1C). All DNAzymes contained either an unmodified catalytic core (no letter L) or a modified core indicated by L^m. [b]In 10 nM RNA and 8 μM DNAzyme. [c]In 10 nM RNA and 100 nM DNAzyme. [d]In 100 nM RNA and 10 nM DNAzyme.

FRS_{GC}9/9. With the FRS_{GU}9/8 DNAzyme series, a 9-fold enhancement in the rate of cleavage was observed (1.5 ± 0.2 and 0.18 ± 0.01 min^{-1}, respectively). However, under multiple-turnover conditions and in some cases (e.g., GAEL9/9I FRS_{GC}9/9), such modification decreased the deoxyribozyme activity. We did not observe reductions in initial cleavage rates, but the percentages of final cleavage with 2′-O-methyl-modified DNAzymes were lower than those obtained with unmodified DNAzymes. Such a loss of efficiency could be due to an increase in the stability of the DNAzyme–RNA substrate complex, which would inhibit product release, reducing multiple-turnover cleavage activity.

To improve nuclease resistance, 2′-O-methyl ribonucleotides were introduced into the catalytic core at nonconserved positions following published guidelines.[14] Under single-turnover conditions and with the exception of FRS_{GC}, the presence of 2′-O-methyl ribonucleotides in the catalytic core reduced deoxyribozyme activity compared to that of DNAzymes with 2′-O-methyl flanking sequences (Table 1). However, under multiple-turnover conditions, $FRS_{GU}9^m$/8^mL^m DNAzyme cleaved faster (1.45 ± 0.02 nM min^{-1}) than unmodified FRS_{GU}9/8 when initial rates of cleavage (v_0) were compared (0.3 ± 0.01 nM min^{-1}). The introduction of six 2′-O-methyl ribonucleotides into the catalytic core of DNAzymes containing 2′-O-methyl ribonucleotides at the end of binding arms slightly decreased the cleavage activity ($FRS_{GC}9^m$/10^mL^m) or increased it ($FRS_{GC}9^m$/9^mL^m and $FRS_{GU}9^m$/8^mL^m) compared to the value of their counterpart with 2′-O-methyl-containing flanking sequences. The estimated values of k_{cat}^{MT} under multiple-turnover conditions obtained after dividing v_0

dx.doi.org/10.1021/bi201532q | Biochemistry 2012, 51, 2181–2191

Table 2. Kinetic Parameters of RNA Cleavage by 2′-O-Methyl-Modified DNAzymes[a]

DNAzyme	target[b]	k_{cat} (min^{-1})	K_m (nM)	k_{cat}/K_m (M^{-1} min^{-1})
GAEL$9^m/9^mI$	25ST-GAEL	0.7 ± 0.1	22.9 ± 6.7	3.06×10^7
GAEL$9^m/9^mIL^m$	25ST-GAEL	0.36 ± 0.02	11.9 ± 2.2	3.02×10^7
$FRS_{GU}9^m/9^m$	24ST-FRS	11.5 ± 0.5	312 ± 37	3.7×10^7
$FRS_{GU}9^m/9^mL^m$	24ST-FRS	5.6 ± 0.2	201 ± 24	2.8×10^7
$FRS_{GU}9^m/9^m$	IGF-I RNA	0.20 ± 0.01	18000 ± 2200	10^4
$FRS_{GU}9^m/9^mL^m$	IGF-I RNA	0.17 ± 0.01	5100 ± 600	3.3×10^4

[a]All kinetic analyses were conducted under single-turnover conditions. [b]Cleavage reactions were performed in 50 mM Tris-HCl (pH 7.5) and 10 mM $MgCl_2$ at 37 °C with synthetic RNA substrate (1 nM) and DNAzyme concentrations from 5 to 200 nM for GAEL and with RNA (10 nM) and DNAzyme concentrations from 50 to 1600 nM for FRS. FRS_{GU} DNAzymes (from 1 to 40 μM) were incubated with a 5′-labeled RNA transcript (100 nM) in 50 mM Tris-HCl (pH 7.5), 200 mM KCl, and 10 mM $MgCl_2$.

by the catalyst concentration (10 nM) were 10 times lower than those obtained under single-turnover conditions (Table 1). DNAzyme inactivation or the presence of competitive secondary structures of target RNA could have an impact on this k_{cat}^{MT}. Moreover, these discrepancies suggested that the slow product release was likely the rate-limiting step at saturating concentrations of the RNA target.[37] However, lower cleavage activities were observed for single and multiple turnovers in the case of FRS_{GU} DNAzymes with longer substrate binding domains ($FRS_{GU}9^m/9^mL^m$ vs $FRS_{GU}9^m/9^m$) and GAEL DNAzymes (GAEL$9^m/9^mIL^m$ vs GAEL$9^m/9^mI$) (Table 1). In both cases, the cleavage rate (k_{cat}) was decreased by half (Table 2). The K_m value also decreased because of the 2′-O-methyl modification in the catalytic core.

In Vitro Cleavage Activities and Specificities of DNAzymes for Rat IGF-I mRNA. A 360-nucleotide fragment of IGF-I mRNA was used to further test DNAzyme cleavage activities. Cleavage reactions were performed under single-turnover conditions with in vitro transcribed RNA and a series of DNAzymes (Figure 2). GAEL and FRS DNAzymes recognized binding sites and induced specific cleavage (Figure 1A). FRS DNAzymes produced expected fragments of 170 and 190 nucleotides, and GAEL DNAzymes produced fragments of 305 and 55 nucleotides.

DNAzyme binding and cleavage efficiency are highly sensitive to RNA secondary structure.[38] We performed an RNase H cleavage assay to determine the accessibility of IGF-I mRNA for binding of complementary oligonucleotides (Figure S3 of the Supporting Information). In vitro transcribed RNA and RNase H were incubated with antisense oligodeoxyribonucleotides fully complementary to IGF-I mRNA and mutated DNAzymes, which were inactivated by a replacement of deoxyguanosine with deoxyadenosine in the catalytic loop.[39] We used these mutated DNAzymes in the RNase H assay to display only the antisense effect due to DNAzyme substrate binding domains. As expected, the RNA cleavage rate was higher with fully complementary duplexes between antisense oligonucleotides and IGF-I RNA. Although the target accessibility for DNAzymes may differ from that for antisense oligonucleotides,[38] we found that the target site accessibility for inactive DNAzyme also decreased in the following order: GAEL ≥ FRS_{GU} > FRS_{GC}. These results were not in agreement with calculated secondary structures of IGF-I mRNA, because the FRS site was expected to be more accessible than the GAEL site (Figure S1 of the Supporting Information). The antisense activity of unmodified mutated DNAzyme was low compared to those of fully complementary antisense oligomers. Indeed, we observed a strong destabilizing effect caused by the loop sequences. The introduction of 2′-O-methyl ribonucleotides to the substrate binding domains greatly improved target binding and RNase H-mediated cleavage efficiencies: MutGAEL$9^m/9^m$ ≥ Mut$FRS_{GU}9^m/9^m$ > Mut$FRS_{GC}9^m/10^m$ (Figure S3 of the Supporting Information). The presence of four 2′-O-methyl ribonucleotides at DNAzyme extremities did not impair RNase H recognition or cleavage.

The DNAzymes of the GAEL and FRS series were then evaluated in a kinetic assay for cleavage of rat IGF-I mRNA (Figure 3). Cleavage rates of GAEL9/9 and GAEL9/9I showed that deoxyinosine insertion enhanced the k_{obs} value nearly 2-fold (Table 3), similar to the increase observed with a short RNA substrate. DNAzymes with 2′-O-methyl ribonucleotides in substrate binding domains exhibited the highest activity. Surprisingly, DNAzymes of the FRS_{GU} series with 2′-O-methyl modifications in the catalytic core, $FRS_{GU}9^m/8^mL^m$ and $FRS_{GU}9^m/9^mL^m$, were more effective (between 1.7- and 2.3-fold) than their counterparts with unmodified cores, $FRS_{GU}9^m/8^m$ and $FRS_{GU}9^m/9^m$ (Table 3 and Figure 3). In contrast, in GAEL series, such modifications interfered with DNAzyme catalytic activity, decreasing k_{obs} 1.4-fold. Catalytic parameters for 2′-O-methyl-containing DNAzymes of FRS_{GU} series were then determined with long IGF-I RNA (Table 2). In contrast with results obtained using a short synthetic RNA substrate, modification in the catalytic core did not decrease the cleavage rate and the improvement in DNAzyme catalytic efficiency was explained by a 3.5-fold decrease in K_m (Table 2).

Comparison of the Intracellular Activities and Specificities of DNAzymes. After selecting the most efficient modified DNAzymes, we validated their cleavage activities in cells using reporter assays. We compared intracellular activities of $FRS_{GU}9^m/9^mL^m$ and $FRS_{GU}9^m/9^m$ that differ only by 2′-O-methyl ribonucleotides in the catalytic loop. We also designed mutated DNAzymes (Mut$FRS_{GU}9^m/9^mQ^m$ and Mut$FRS_{GU}9^m/9^m$) that were unable to cleave because of replacement of the essential deoxyguanosine with deoxyadenosine in the catalytic core.[39] The binding affinities of mutated inactive DNAzymes on a noncleavable complementary target were similar to those of their active counterpart (Table 4). The control DNAzyme had an intact catalytic loop but scrambled hybridization arms.

We cotransfected DNAzymes with psick-rIGF1(1833)ΔFluc, a plasmid in which rat IGF-I cDNA was fused to *Renilla* luciferase (Figure 4). After $FRS_{GU}9^m/9^mL^m$ DNAzyme transfection, hR-Luc was reduced by 40−50% in comparison with samples treated with mutated and scrambled DNAzyme controls. A comparison with its inactive mutated counterpart, Mut$FRS_{GU}9^m/9^mQ^m$, suggested that this FRS_{GU} DNAzyme was able to cleave IGF-I/hR-Luc RNA in cells and led to specific

dx.doi.org/10.1021/bi201532q | *Biochemistry* 2012, 51, 2181−2191

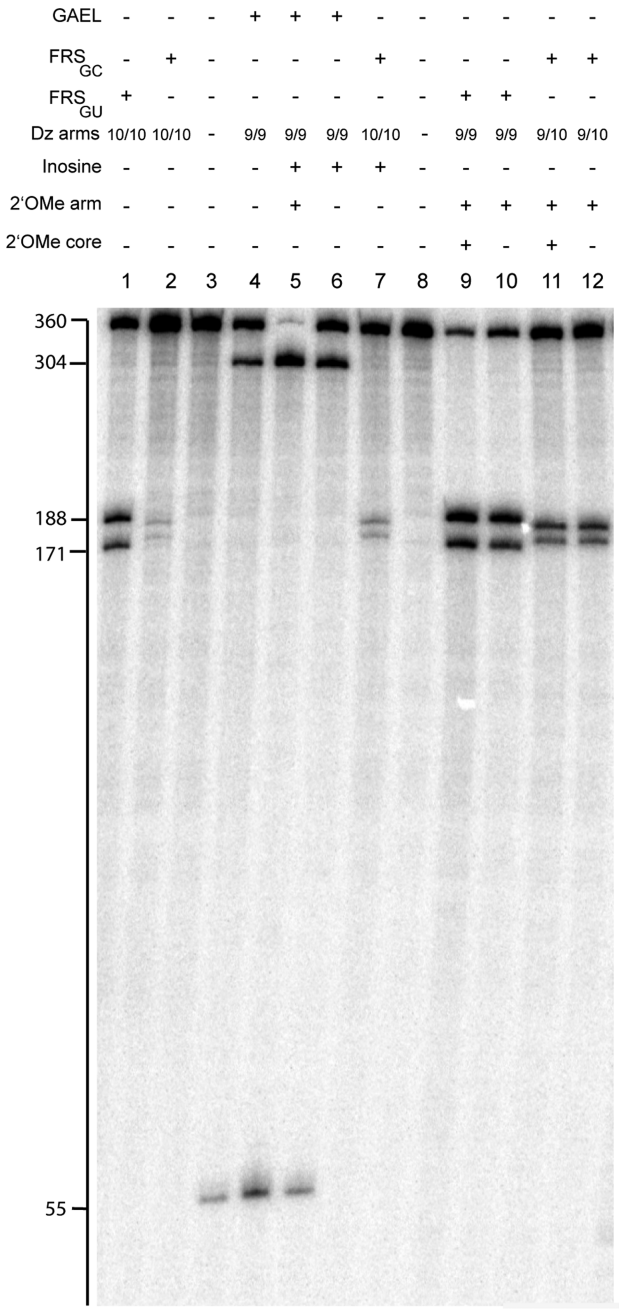

Figure 2. Cleavage of in vitro transcribed IGF-I mRNA by DNAzymes. Cleavage product analysis using denaturing PAGE shows that DNAzymes induced specific cleavage of internally radiolabeled RNA with various efficacies. Predicted fragment sizes are indicated. GAEL and FRS series gave two products. Deoxyinosine and 2′-O-methyl nucleotides in the flanking sequences and catalytic core are indicated. In vitro transcribed RNA (0.02 μM) was incubated for 4.5 h at 37 °C with 1 μM DNAzyme in 50 mM Tris-HCl buffer (pH 7.5) containing 10 mM $MgCl_2$. Lanes 3 and 8 show radiolabeled RNA controls.

luciferase inhibition. Surprisingly, $FRS_{GU}9^m/9^m$ DNAzyme with no 2′-O-methyl modifications in the catalytic loop but with 2′-O-methyl-flanking sequences was unable to inhibit luciferase activity. The $FRS_{GU}9^m/9^m$ DNAzyme catalytic efficiency was 3 times lower than for $FRS_{GU}9^m/9^mL^m$, suggesting that only efficient catalytic 10−23 DNAzyme can achieve gene inhibition in cells.

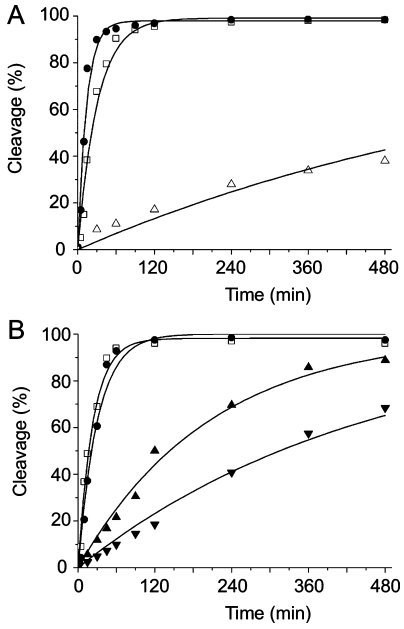

Figure 3. Time courses of IGF-I RNA cleavage by modified DNAzymes. (A) RNA cleavage kinetic analysis obtained with DNAzymes targeting the FRS site: $FRS_{GU}10/10$ (△), $FRS_{GU}9^m/9^m$ (□), and $FRS_{GU}9^m/9^mL^m$ (●). (B) Cleavage kinetic analysis of DNAzymes targeted to GAEL: GAEL9/9 (▼), GAEL9/9I (▲), $GAEL9^m/9^mI$ (□), and $GAEL9^m/9^mIL^m$ (●). The 360-nucleotide IGF-I RNA (0.1 μM) was incubated with DNAzymes (5 μM) at 37 °C in 50 mM Tris-HCl (pH 7.5), 10 mM $MgCl_2$, and 200 mM KCl. Solid lines represent least-squares fits of experimental data using Origin and equations described in Experimental Procedures.

Table 3. Rates of Cleavage of DNAzymes on Rat IGF-I mRNA[a]

DNAzyme	k_{obs} (min^{-1})
GAEL9/9	0.0024 ± 0.0001
GAEL9/9I	0.0048 ± 0.0003
$GAEL9^m/9^mI$	0.043 ± 0.004
$GAEL9^m/9^mIL^m$	0.033 ± 0.002
$FRS_{GC}9^m/10^m$	0.00067 ± 0.00007
$FRS_{GC}9^m/10^mL^m$	0.00064 ± 0.00005
$FRS_{GU}10/10$	0.0012 ± 0.0001
$FRS_{GU}9^m/8^m$	0.0036 ± 0.0006
$FRS_{GU}9^m/8^mL^m$	0.010 ± 0.001
$FRS_{GU}9^m/9^m$	0.032 ± 0.004
$FRS_{GU}9^m/9^mL^m$	0.073 ± 0.009

[a]Cleavage reactions were performed in 50 mM Tris-HCl (pH 7.5), 10 mM $MgCl_2$, and 200 mM KCl at 37 °C with in vitro transcribed 5′-labeled RNA substrate (100 nM) and DNAzymes (5 μM).

Table 4. Stabilities of DNAzymes on a Short RNA Target[a]

DNAzyme	C_{50} (nM)
$FRS_{GU}9^m/9^m$	19.2 ± 2.8
$MutFRS_{GU}9^m/9^m$	15.1 ± 1.9
$FRS_{GU}9^m/9^mL^m$	22.8 ± 3.2
$MutFRS_{GU}9^m/9^m$ Q^m	25 ± 3.7

[a]Increasing concentrations of DNAzymes (from 10 to 250 nM) were incubated at 37 °C with a noncleavable short RNA target, NC-FRS (38 nM), and analyzed by native gel electrophoresis. C_{50} represents the concentration of DNAzymes at which 50% of the complex was formed.

dx.doi.org/10.1021/bi201532q | *Biochemistry* 2012, 51, 2181−2191

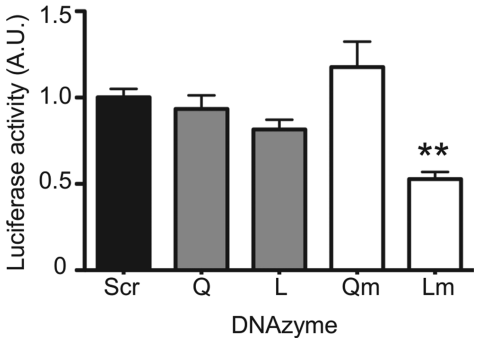

Figure 4. Functional validation of intracellular cleavage activities of DNAzymes. DNAzymes (150 ng, 50 nM) were cotransfected in LFCL2A rat hepatocarcinoma cells with psick-rIGF1(1833)ΔFluc (100 ng, 100 pM) and pGL2-CMV (25 ng, 28 pM). Cells were harvested and luciferase activities measured 24 h post-transfection. Plasmids were cell-transfected with control DNAzyme (Scr), MutFRS$_{GU}$9^{m}/9^{m} (Q), FRS$_{GU}$9^{m}/9^{m} (L), MutFRS$_{GU}$9^{m}/9^{m}Q^{m} (Qm), or FRS$_{GU}$9^{m}/9^{m}L^{m} (Lm). Data are means of four independent experiments ± SEM. $^{**}P < 0.01$ refers to a comparison to Scr.

DISCUSSION

Several approaches using nucleic acids to downregulate cellular IGF-I or IGF-IR expression have been developed, such as antisense oligonucleotides or short interfering RNAs. Here, we designed a series of 10−23 DNAzymes to target IGF-I mRNA in tumor cells. We found that increasing the length of DNAzyme substrate binding domains from 8 to 10 nucleotides improved the cleavage efficiency of target RNAs. This is in accordance with the literature; previous studies demonstrated that DNAzyme arms longer than 9 or 10 nucleotides may be detrimental because of the decreased rate of turnover as a consequence of slow dissociation of products from DNAzyme.[6,40] Unmodified DNAzymes are prone to nucleolytic degradation in biological media. Several modifications, such as 2′-O-methyl ribonucleotides or a 3′−3′ inverted thymidine at the 3′ end, have been successfully used to protect DNAzyme extremities from nucleolytic degradation.[8,41,42] Although these modifications increase the nuclease resistance of DNAzymes, they also influence their catalytic activity, either positively by strengthening binding to structured RNA targets or negatively by interfering with the cleaved product release rates.[43] In our study, we introduced 2′-O-methyl nucleosides first into DNAzyme substrate binding domains and then into the catalytic core. We replaced four deoxyribonucleotides in the substrate binding domains with 2′-O-methyl analogues to increase the DNAzyme half-life in cells.[14] This modification increased the cleavage efficiency of short RNAs and long IGF-I mRNA. We also introduced six 2′-O-methyl modifications at the nonconservative positions of the IGF-I DNAzyme catalytic core. This substitution was expected to improve 10−23 DNAzyme stability and reduce endonucleolytic degradation, without a substantial loss of catalytic activity.[14,39] These modifications of IGF-I DNAzymes either had no effect (FRS$_{GC}$) or resulted in a decrease in catalytic activity when studied on short RNA fragments. A reduction in cleavage efficiency was observed with DNAzymes GAEL9^{m}/9^{m}IL^{m} and FRS$_{GU}$9^{m}/9^{m}L^{m}, whereas in the case of activity on the long IGF-I mRNA substrate, we observed a slight inhibition of GAEL9^{m}/9^{m}IL^{m} activity and a near 2-fold enhancement of the observed cleavage rate for DNAzyme FRS$_{GU}$9^{m}/9^{m}L^{m}.

Kinetic parameters of GAEL9^{m}/9^{m}IL^{m} and FRS$_{GU}$9^{m}/9^{m}L^{m} were then analyzed on both targets. A large excess of DNAzyme was used on short target RNAs to determine k_{cleav} values: under such conditions, the chemical cleavage reaction was the limiting step. Interestingly, the k_{cat} values were equivalent to k_{cleav} values and thus can be considered as the true cleavage rate. Insertion of 2′-O-methyl nucleotides into the DNAzyme catalytic core inhibited the cleavage rate; we assume that this modification led to distortion of the favorable active conformation of the DNAzyme−RNA substrate complex. In contrast, we did not observe such a decrease in the cleavage efficiency of the long IGF-I transcript because of the presence of 2′-O-methyl nucleotides in the catalytic core in the case of FRS$_{GU}$9^{m}/9^{m}L^{m}. Here, the k_{obs} parameter cannot be considered as the true cleavage rate of the phosphodiester bond of the structured long RNA target, because conformational changes of the DNAzyme−RNA complex are mandatory for efficient cleavage catalysis. The formation of an active DNAzyme−RNA complex was the limiting step of the reaction.

The DNAzyme catalytic loop plays a critical role in folding of the DNAzyme−RNA complex, and therefore, the presence of 2′-O-methyl-modified nucleotides in the core may contribute to stabilization of the active conformation and to cleavage reactivity by inducing favorable kinks in the mRNA−DNAzyme complex. The extent of kinking will depend on bulged nucleotides and on the sequence of the flanking base pairs. The loop may generate kinks inducing a favorable in-line conformation of the cleavable RNA phosphodiester bond.[44] Some knowledge about the structure of the catalytic core of active 10−23 DNAzyme is available.[45−47] Upon binding, the DNAzyme bends its RNA substrate away from the cleavage point, exposing the reactive site to the DNAzyme catalytic core.[48,49] Such bending can induce enough stretch to partially unstack the unpaired base in the DNAzyme−RNA complex. Using a coarse-grained Brownian dynamics simulation, it was shown that mutations in the catalytic core changed the bending angle, but no correlation was found with DNAzyme catalytic activities. Central nucleotides (C7−A12) in catalytic core could provide a scaffold that keeps the key bases for catalysis (G1, G2, T4, G6, and G14) in the proximity of the cleavage site (Figure 1C).[49] In the case of short RNA targets, we assume that 2′-O-methyl nucleotides in the DNAzyme catalytic core led to less favorable bending of the substrate. When nucleotides in the central part of the catalytic core are 2′-O-methyl analogues, the catalytically preferred conformation of the DNAzyme bound to short RNAs may be destabilized. The DNAzyme catalytic efficiency of FRS$_{GU}$9^{m}/9^{m}L^{m} had a nearly 3-fold lower K_m value compared to that of FRS$_{GU}$9^{m}/9^{m} in the reaction with IGF-I RNA (Table 2). This was likely due to an increase in the stability of the DNAzyme−RNA complex and to a favorable folding to obtain efficient binding induced by the presence of 2′-O-methyl modifications in the catalytic core.

The design of efficient antisense oligonucleotides, short interfering RNA, or nucleic acid enzymes such as DNAzymes and hammerhead ribozymes is usually guided by the accessibility of the target site. To help the design of efficient antisense oligomers, a number of theoretical and practical approaches have been developed to identify accessible regions in these RNAs.[50] For example, efficient DNAzymes have been identified from combinatorial libraries or oligonucleotide scanning arrays.[51,52] In the case of rat IGF-I mRNA, we identified two target sites using in silico prediction with specific folding algorithms that could be hybridized in vitro in the

absence of intracellular proteins. An estimate of target site accessibility may also be obtained from RNase H assays. In our system, the FRS sites were predicted to be more hybridizable than the GAEL site. Nevertheless, RNase H induced more efficient cleavage on the duplexes formed by GAEL DNAzyme and IGF-I mRNA, in contrast with what was expected if we considered only accessibility. Therefore, it was difficult to determine whether differences in cleavage efficiency were due to RNase H, which does display minimal sequence preferences for certain nucleotide stretches formed upon binding to mRNA target, or to thermodynamic stabilities of displaced secondary structures that differed from that predicted. As expected, we found that DNAzymes with 2′-O-methyl-modified arms led to a better cleavage rate of IGF-I mRNA as compared to those of unmodified DNAzymes, confirming the important role of 2′-O-methyl nucleotides in disrupting local secondary structures. Divalent metal ions such as Mg^{2+} play a dual role in 10−23 DNAzyme catalysis, because they stabilize folded RNA structures and the active conformation of DNAzymes and are also essential for efficient cleavage of RNA phosphodiester bonds. Most of the in vitro studies of 10−23 DNAzymes have used Mg^{2+} concentrations ranging from 10 to 25 mM, much higher than the concentration of 0.5 mM available in cells.[53] Several groups have isolated new DNAzymes that cleave RNA in the presence of low concentrations of Mg^{2+} or in the absence of Mg^{2+} using SELEX procedures in the presence of synthetic nucleotides bearing reactive groups able to cleave RNA.[54−56] Structural requirements and mechanisms of these new DNAzymes have been explored in vitro. These Mg^{2+}-independent DNAzymes have not yet been evaluated in cells, but they may represent interesting alternatives for degrading mRNA. Recently, it was shown that 10−23 DNAzymes have a very weak Mg^{2+} ion dependence, with DNAzyme activity observed at 0.01 mM Mg^{2+}.[57] Therefore, we investigated if DNAzymes can cleave a short complementary target under physiological conditions of 0.5 mM Mg^{2+}, 150 mM NaCl, pH 7.4, and 37 °C.[58] Our results confirmed that modified FRS_{GU} DNAzymes were able to cleave their RNA target under these conditions, but to a lesser extent as compared to conditions with 10 mM Mg^{2+} (Table S3 of the Supporting Information). Consequently, because modified FRS_{GU} DNAzymes exhibited cleavage activity under physiological conditions, we can expect that RNA cleavage occurs also in cells.

The effect of anti-IGF-I DNAzymes was analyzed using transient transfection assays with reporter plasmids.[18,59] We demonstrated that $FRS_{GU}9^m/9^mL^m$ DNAzyme was able to inhibit reporter activity upon recognition of its target on IGF-I mRNA fused to *R. reniformis* luciferase. In previous cell studies, several DNAzyme controls were used: a scrambled control with arms of unrelated sequences, a DNAzyme with a reverse catalytic core sequence, a mismatch control in which a base is changed in the flanking sequences, and a mutated core control in which a nucleotide in the catalytic loop is replaced to inactivate cleavage activity.[43] The observed inhibition obtained with $FRS_{GU}9^m/9^mL^m$ was sequence-specific because a DNAzyme with scrambled flanking arms did not inhibit luciferase activity. Results obtained with the mutated core control strongly suggest that $FRS_{GU}9^m/9^mL^m$ inhibited luciferase activity through the induction of RNA cleavage. It is difficult to determine why $FRS_{GU}9^m/9^m$, its counterpart without a modified catalytic loop, has no effect in cells. The catalytic activities of $FRS_{GU}9^m/9^m$ measured in vitro may not be sufficiently high to provide efficient cleavage. $FRS_{GU}9^m/9^m$ DNAzyme might be more sensitive to nucleases than $FRS_{GU}9^m/9^mL^m$.[14] We can also hypothesize that folding of $FRS_{GU}9^m/9^m$ in cells was not appropriate for inducing RNA cleavage, in contrast to $FRS_{GU}9^m/9^mL^m$, which likely exhibited constraint in its catalytic core due to the six 2′-O-methyl ribonucleotides. DNAzyme approaches have been successfully applied in cells and in vivo; however, their inhibitory mechanisms were often unexplored.[8,43] Cellular cleavage activities of nucleic acid enzymes such as ribozymes were previously supported by the use of inactive mutants that exhibited weak inhibitory effects.[60,61] Moreover, the biological action of ribozymes or 10−23 DNAzyme could be mainly caused by the antisense effect of substrate binding domains.[26,48] A recent comparison of catalytically active and inactive 10−23 DNAzymes harboring large DNA flanking sequences (>12 nucleotides) suggested that the inhibitory mechanism was mainly mediated by RNase H recognition and cleavage of DNAzyme−RNA complexes in cells.[62] It was also shown that some 10−23 DNAzyme activities were due to cytotoxicity or to the presence of specific motifs such as a G-rich stretch.[63] In cells, RNase H that recognizes flanking sequences bound to mRNA can contribute to the inhibition observed with IGF-I DNAzymes (Figure S3 of the Supporting Information), provided that they contained desoxyribonucleotides and not 2′-O-methyl-RNA nucleotides. The stability of complexes formed between RNA targets and mutated DNAzymes was similar to the stability of those formed with active DNAzymes (Table 4). Moreover, RNA−DNA complexes formed by active and inactive DNAzymes differing by only one nucleotide in the catalytic loop were equally sensitive to *Escherichia coli* RNase H cleavage activity (data not shown), suggesting that RNase H may cleave mRNA in cells with the same efficiency when bound to active or mutated DNAzymes. One example for that was mRNA complexes formed with $FRS_{GU}9^m/9^mL^m$ or $MutFRS_{GU}9^m/9^mQ^m$. Our results obtained with two DNAzyme controls, one with a mutated catalytic core and the other with scrambled flanking arms, strongly suggest that the 2′-O-methyl nucleotide-containing active DNAzyme specifically recognized its RNA target and cleaved it in a Mg^{2+}-dependent manner in cells. The cellular RNase H likely contributed to the observed inhibition. However, the presence of an active catalytic core in DNAzyme improved the inhibition as compared to its inactive counterpart. Further studies are needed to unravel inhibitory mechanisms, for instance, via analysis of cellular cleavage products after transfection of cells silenced for RNase H.[64] Indeed, the ubiquitous RNase H could be transiently knocked down using specific short interfering RNA.[65−67] Transfection of DNAzymes in cells devoid of ribonuclease H would allow determination of the relative contribution of protein-free DNAzyme and ribonuclease H catalysis to the observed inhibition.

Here, efficient 10−23 DNAzymes with 2′-O-methyl nucleotides in flanking sequences and in the catalytic core were identified to cleave rat IGF-I mRNA in vitro and subsequently were shown to inhibit specifically the expression of a reporter gene fused to IGF-I mRNA. These modified DNAzymes could be useful for blocking the secretion of IGF-I from prostate stroma primary cells and may inhibit prostate tumor development as previously shown using siRNA transfection.[68,69] As for neutralizing antibodies, we can expect to block hepatic metastasis by inhibiting the expression of IGF-I in liver, which is the major source of serum IGF-I.[70] The development of these modified 10−23 DNAzymes, which were effective against IGF-I

mRNA, opens opportunities to inhibit IGF-I expression in tumor models and to explore its role in tumorigenesis and immune response triggering.[21]

■ ASSOCIATED CONTENT

Supporting Information

Target RNAs and DNAzymes (Table S1), catalytic activities of deoxyinosine-containing DNAzymes (Table S2), effect of decreasing Mg^{2+} concentration on DNAzyme catalytic activities (Table S3), predicted secondary structure of rat IGF-I mRNA (Figure S1), cDNA sequence comparison of IGF-I and related proteins (Figure S2), and accessibility of target sites on IGF-I RNA via an RNase H assay (Figure S3). This material is available free of charge via the Internet at http://pubs.acs.org.

■ AUTHOR INFORMATION

Corresponding Author

*Telephone: +33 1 40 79 38 01. Fax: +33 1 40 79 37 05. E-mail: jean-christophe.francois@inserm.fr.

Present Address

[⊥]INSERM-UPMC, UMR S938, CDR Saint-Antoine, Hôpital Saint-Antoine, Paris, France.

Funding

This work was supported by Grant 03-51-5281 from INTAS (International Association for the promotion of cooperation with scientists from the new independent states of the former Soviet Union, Brussels, Belgium), Hubert Curien Partnership 18908VK, and Russian State Program RI-111/002/097. A.A.F. benefits from a fellowship of FEBS and T.D. from a doctoral fellowship from the Ministère délégué à l'enseignement supérieur et à la recherche (France) and Ligue Nationale Contre le Cancer (France).

Notes

The authors declare no competing financial interest.

■ ACKNOWLEDGMENTS

We thank Dr. Christiane Frayssinet for rat IGF-I cDNA and rat hepatocarcinoma cell line LFCL2A, Prof. Alexandre Boutorine and Dr. Martin Holzenberger for critical discussion, and Arnaud Defaye and Nolwenn Lucas for technical assistance.

■ ABBREVIATIONS

RNase H, ribonuclease H; RISC, RNA-induced silencing complex; DNAzyme, deoxyribozyme; 2′-O-Me, 2′-O-methyl ribonucleotide; PAGE, polyacrylamide gel electrophoresis; SELEX, systematic evolution of ligands by exponential enrichment.

■ REFERENCES

(1) Rayburn, E. R., and Zhang, R. (2008) Antisense, RNAi, and gene silencing strategies for therapy: Mission possible or impossible? *Drug Discovery Today 13*, 513−521.

(2) Bauman, J., Jearawiriyapaisarn, N., and Kole, R. (2009) Therapeutic potential of splice-switching oligonucleotides. *Oligonucleotides 19*, 1−13.

(3) Corey, D. R. (2007) RNA learns from antisense. *Nat. Chem. Biol.* 3, 8−11.

(4) Scott, W. G. (2007) Ribozymes. *Curr. Opin. Struct. Biol. 17*, 280−286.

(5) Baum, D. A., and Silverman, S. K. (2008) Deoxyribozymes: Useful DNA catalysts in vitro and in vivo. *Cell. Mol. Life Sci. 65*, 2156−2174.

(6) Santoro, S. W., and Joyce, G. F. (1998) Mechanism and utility of an RNA-cleaving DNA enzyme. *Biochemistry 37*, 13330−13342.

(7) Schlosser, K., and Li, Y. (2009) Biologically inspired synthetic enzymes made from DNA. *Chem. Biol. 16*, 311−322.

(8) Isaka, Y. (2007) DNAzymes as potential therapeutic molecules. *Curr. Opin. Mol. Ther. 9*, 132−136.

(9) Cairns, M. J., King, A., and Sun, L. Q. (2003) Optimisation of the 10−23 DNAzyme-substrate pairing interactions enhanced RNA cleavage activity at purine-cytosine target sites. *Nucleic Acids Res. 31*, 2883−2889.

(10) Asanuma, H., Hayashi, H., Zhao, J., Liang, X., Yamazawa, A., Kuramochi, T., Matsunaga, D., Aiba, Y., Kashida, H., and Komiyama, M. (2006) Enhancement of RNA cleavage activity of 10−23 DNAzyme by covalently introduced intercalator. *Chem. Commun.*, 5062−5064.

(11) Wu, Y., Yu, L., McMahon, R., Rossi, J. J., Forman, S. J., and Snyder, D. S. (1999) Inhibition of bcr-abl oncogene expression by novel deoxyribozymes (DNAzymes). *Hum. Gene Ther. 10*, 2847−2857.

(12) Cieslak, M., Niewiarowska, J., Nawrot, M., Koziolkiewicz, M., Stec, W. J., and Cierniewski, C. S. (2002) DNAzymes to β1 and β3 mRNA down-regulate expression of the targeted integrins and inhibit endothelial cell capillary tube formation in fibrin and matrigel. *J. Biol. Chem. 277*, 6779−6787.

(13) Schubert, S., Furste, J. P., Werk, D., Grunert, H. P., Zeichhardt, H., Erdmann, V. A., and Kurreck, J. (2004) Gaining target access for deoxyribozymes. *J. Mol. Biol. 339*, 355−363.

(14) Schubert, S., Gul, D. C., Grunert, H. P., Zeichhardt, H., Erdmann, V. A., and Kurreck, J. (2003) RNA cleaving '10−23' DNAzymes with enhanced stability and activity. *Nucleic Acids Res. 31*, 5982−5992.

(15) Wiktorska, M., Papiewska-Pajak, I., Okruszek, A., Sacewicz-Hofman, I., and Niewiarowska, J. (2010) DNAzyme as an efficient tool to modulate invasiveness of human carcinoma cells. *Acta Biochim. Pol. 57*, 269−275.

(16) Takahashi, H., Hamazaki, H., Habu, Y., Hayashi, M., Abe, T., Miyano-Kurosaki, N., and Takaku, H. (2004) A new modified DNA enzyme that targets influenza virus A mRNA inhibits viral infection in cultured cells. *FEBS Lett. 560*, 69−74.

(17) Fluiter, K., Frieden, M., Vreijling, J., Koch, T., and Baas, F. (2005) Evaluation of LNA-modified DNAzymes targeting a single nucleotide polymorphism in the large subunit of RNA polymerase II. *Oligonucleotides 15*, 246−254.

(18) Jakobsen, M. R., Haasnoot, J., Wengel, J., Berkhout, B., and Kjems, J. (2007) Efficient inhibition of HIV-1 expression by LNA modified antisense oligonucleotides and DNAzymes targeted to functionally selected binding sites. *Retrovirology 4*, 29.

(19) Vester, B., Hansen, L. H., Lundberg, L. B., Babu, B. R., Sorensen, M. D., Wengel, J., and Douthwaite, S. (2006) Locked nucleoside analogues expand the potential of DNAzymes to cleave structured RNA targets. *BMC Mol. Biol. 7*, 19.

(20) Baserga, R. (2005) The insulin-like growth factor-I receptor as a target for cancer therapy. *Expert Opin. Ther. Targets 9*, 753−768.

(21) Lafarge-Frayssinet, C., Duc, H. T., Frayssinet, C., Sarasin, A., Anthony, D., Guo, Y., and Trojan, J. (1997) Antisense insulin-like growth factor I transferred into a rat hepatoma cell line inhibits tumorigenesis by modulating major histocompatibility complex I cell surface expression. *Cancer Gene Ther. 4*, 276−285.

(22) Schillaci, R., Salatino, M., Cassataro, J., Proietti, C. J., Giambartolomei, G. H., Rivas, M. A., Carnevale, R. P., Charreau, E. H., and Elizalde, P. V. (2006) Immunization with murine breast cancer cells treated with antisense oligodeoxynucleotides to type I insulin-like growth factor receptor induced an antitumoral effect mediated by a CD8+ response involving Fas/Fas ligand cytotoxic pathway. *J. Immunol. 176*, 3426−3437.

(23) Shaw, L. C., Pan, H., Afzal, A., Calzi, S. L., Spoerri, P. E., Sullivan, S. M., and Grant, M. B. (2006) Proliferating endothelial cell-specific expression of IGF-I receptor ribozyme inhibits retinal neovascularization. *Gene Ther. 13*, 752−760.

(24) Oussedik, K., François, J. C., Halby, L., Senamaud-Beaufort, C., Toutirais, G., Dallavalle, S., Pommier, Y., Pisano, C., and Arimondo, P. B. (2010) Sequence-specific targeting of IGF-I and IGF-IR genes by camptothecins. *FASEB J. 24*, 2235−2244.
(25) Lecosnier, S., Cordier, C., Simon, P., François, J. C., and Saison-Behmoaras, T. E. (2011) A steric blocker of translation elongation inhibits IGF-1R expression and cell transformation. *FASEB J. 25*, 2201−2210.
(26) Guo, N., Ye, J. J., Liang, S. J., Mineo, R., Li, S. L., Giannini, S., Plymate, S. R., Sikes, R. A., and Fujita-Yamaguchi, Y. (2003) The role of insulin-like growth factor-II in cancer growth and progression evidenced by the use of ribozymes and prostate cancer progression models. *Growth Horm. IGF Res. 13*, 44−53.
(27) Durfort, T., Tkach, M., Meschaninova, M., Rivas, M., Elizalde, P., Venyaminova, A., Schillaci, R., and François, J. C. (2012) Small Interfering RNA Targeted to IGF-IR Delays Tumor Growth and Induces Proinflammatory Cytokines in a Mouse Breast Cancer Model. *PLoS One 7*, e29213.
(28) Chen, Z., Ge, Y., and Kang, J. X. (2004) Down-regulation of the M6P/IGF-II receptor increases cell proliferation and reduces apoptosis in neonatal rat cardiac myocytes. *BMC Cell Biol. 5*, 15.
(29) Bohula, E. A., Salisbury, A. J., Sohail, M., Playford, M. P., Riedemann, J., Southern, E. M., and Macaulay, V. M. (2003) The efficacy of small interfering RNAs targeted to the type 1 insulin-like growth factor receptor (IGF1R) is influenced by secondary structure in the IGF1R transcript. *J. Biol. Chem. 278*, 15991−15997.
(30) Murphy, L. J., Bell, G. I., Duckworth, M. L., and Friesen, H. G. (1987) Identification, characterization, and regulation of a rat complementary deoxyribonucleic acid which encodes insulin-like growth factor-I. *Endocrinology 121*, 684−691.
(31) Hassani, Z., François, J. C., Alfama, G., Dubois, G. M., Paris, M., Giovannangeli, C., and Demeneix, B. A. (2007) A hybrid CMV-H1 construct improves efficiency of PEI-delivered shRNA in the mouse brain. *Nucleic Acids Res. 35*, e65.
(32) Kuo, W. W., Liu, C. J., Chen, L. M., Wu, C. H., Chu, C. H., Liu, J. Y., Lu, M. C., Lin, J. A., Lee, S. D., and Huang, C. Y. (2006) Cardiomyoblast apoptosis induced by insulin-like growth factor (IGF)-I resistance is IGF-II dependent and synergistically enhanced by angiotensin II. *Apoptosis 11*, 1075−1089.
(33) Pecha, J., Ankrapp, D., Jiang, C., Tang, W., Hoshino, I., Bruck, K., Wagner, K. U., and Xiao, H. (2007) Deletion of Tip30 leads to rapid immortalization of murine mammary epithelial cells and ductal hyperplasia in the mammary gland. *Oncogene 26*, 7423−7431.
(34) Yokota, T., Shimokawa, H., Shibata, S., Itoh, K., Baba, Y., Ohya, K., Ohyama, K., and Suzuki, S. (2008) Insulin-like growth factor I regulates apoptosis in condylar cartilage. *J. Dent. Res. 87*, 159−163.
(35) Sun, L. Q., Cairns, M. J., Gerlach, W. L., Witherington, C., Wang, L., and King, A. (1999) Suppression of smooth muscle cell proliferation by a c-myc RNA-cleaving deoxyribozyme. *J. Biol. Chem. 274*, 17236−17241.
(36) Sugimoto, N., Nakano, S., Katoh, M., Matsumura, A., Nakamuta, H., Ohmichi, T., Yoneyama, M., and Sasaki, M. (1995) Thermodynamic parameters to predict stability of RNA/DNA hybrid duplexes. *Biochemistry 34*, 11211−11216.
(37) Ting, R., Thomas, J. M., Lermer, L., and Perrin, D. M. (2004) Substrate specificity and kinetic framework of a DNAzyme with an expanded chemical repertoire: A putative RNaseA mimic that catalyzes RNA hydrolysis independent of a divalent metal cation. *Nucleic Acids Res. 32*, 6660−6672.
(38) Kurreck, J., Bieber, B., Jahnel, R., and Erdmann, V. A. (2002) Comparative study of DNA enzymes and ribozymes against the same full-length messenger RNA of the vanilloid receptor subtype I. *J. Biol. Chem. 277*, 7099−7107.
(39) Zaborowska, Z., Furste, J. P., Erdmann, V. A., and Kurreck, J. (2002) Sequence requirements in the catalytic core of the "10−23" DNA enzyme. *J. Biol. Chem. 277*, 40617−40622.
(40) Ackermann, J. M., Kanugula, S., and Pegg, A. E. (2005) DNAzyme-mediated silencing of ornithine decarboxylase. *Biochemistry 44*, 2143−2152.
(41) Kurreck, J. (2003) Antisense technologies. Improvement through novel chemical modifications. *Eur. J. Biochem. 270*, 1628−1644.
(42) Kuznetsova, M., Fokina, A., Lukin, M., Repkova, M., Venyaminova, A., and Vlassov, V. (2003) Catalytic DNA and RNA for targeting MDR1 mRNA. *Nucleosides, Nucleotides Nucleic Acids 22*, 1521−1523.
(43) Dass, C. R., Choong, P. F., and Khachigian, L. M. (2008) DNAzyme technology and cancer therapy: Cleave and let die. *Mol. Cancer Ther. 7*, 243−251.
(44) Soukup, G. A., and Breaker, R. R. (1999) Relationship between internucleotide linkage geometry and the stability of RNA. *RNA 5*, 1308−1325.
(45) Wang, B., Cao, L., Chiuman, W., Li, Y., and Xi, Z. (2010) Probing the function of nucleotides in the catalytic cores of the 8−17 and 10−23 DNAzymes by abasic nucleotide and C3 spacer substitutions. *Biochemistry 49*, 7553−7562.
(46) Nawrot, B., Widera, K., Wojcik, M., Rebowska, B., Nowak, G., and Stec, W. J. (2007) Mapping of the functional phosphate groups in the catalytic core of deoxyribozyme 10−23. *FEBS J. 274*, 1062−1072.
(47) Nowakowski, J., Shim, P. J., Prasad, G. S., Stout, C. D., and Joyce, G. F. (1999) Crystal structure of an 82-nucleotide RNA-DNA complex formed by the 10−23 DNA enzyme. *Nat. Struct. Biol. 6*, 151−156.
(48) Cieslak, M., Szymanski, J., Adamiak, R. W., and Cierniewski, C. S. (2003) Structural rearrangements of the 10−23 DNAzyme to β3 integrin subunit mRNA induced by cations and their relations to the catalytic activity. *J. Biol. Chem. 278*, 47987−47996.
(49) Kenward, M., and Dorfman, K. D. (2009) Coarse-Grained Brownian Dynamics Simulations of the 10−23 DNAzyme. *Biophys. J. 97*, 2785−2793.
(50) Lutzelberger, M., and Kjems, J. (2006) Strategies to identify potential therapeutic target sites in RNA. *Handb. Exp. Pharmacol.,* 243−259.
(51) Doran, G., and Sohail, M. (2006) Systematic analysis of the role of target site accessibility in the activity of DNA enzymes. *J. RNAi Gene Silencing 2*, 205−214.
(52) Kim, K., Choi, W., Gong, S., Oh, S., Kim, J., and Kim, D. (2006) Efficient target site selection for an RNA-cleaving DNAzyme through combinatorial library screening. *Bull. Korean Chem. Soc. 27*, 657−662.
(53) Romani, A. M., and Scarpa, A. (2000) Regulation of cellular magnesium. *Front. Biosci. 5*, D720−D734.
(54) Franzen, S. (2010) Expanding the catalytic repertoire of ribozymes and deoxyribozymes beyond RNA substrates. *Curr. Opin. Mol. Ther. 12*, 223−232.
(55) Hollenstein, M., Hipolito, C. J., Lam, C. H., and Perrin, D. M. (2009) A DNAzyme with three protein-like functional groups: Enhancing catalytic efficiency of M^{2+}-independent RNA cleavage. *ChemBioChem 10*, 1988−1992.
(56) Kuwahara, M., and Sugimoto, N. (2010) Molecular evolution of functional nucleic acids with chemical modifications. *Molecules 15*, 5423−5444.
(57) Ruble, B., Richards, J., Cheung-Lau, J., and Dmochowski, I. (2011) Mismatch discrimination and efficient photomodulation with split 10−23 DNAzymes. *Inorg. Chim. Acta*, DOI: 10.1016/j.ica.2011.10.068.
(58) Lam, C. H., and Perrin, D. M. (2010) Introduction of guanidinium-modified deoxyuridine into the substrate binding regions of DNAzyme 10−23 to enhance target affinity: Implications for DNAzyme design. *Bioorg. Med. Chem. Lett. 20*, 5119−5122.
(59) Cairns, M. J., Saravolac, E. G., and Sun, L. Q. (2002) Catalytic DNA: A novel tool for gene suppression. *Curr. Drug Targets 3*, 269−279.
(60) Shaw, L. C., Afzal, A., Lewin, A. S., Timmers, A. M., Spoerri, P. E., and Grant, M. B. (2003) Decreased expression of the insulin-like growth factor 1 receptor by ribozyme cleavage. *Invest. Ophthalmol. Visual Sci. 44*, 4105−4113.
(61) Xu, Z. D., Oey, L., Mohan, S., Kawachi, M. H., Lee, N. S., Rossi, J. J., and Fujita-Yamaguchi, Y. (1999) Hammerhead ribozyme-mediated

cleavage of the human insulin-like growth factor-II ribonucleic acid in vitro and in prostate cancer cells. *Endocrinology 140*, 2134−2144.
(62) Young, D. D., Lively, M. O., and Deiters, A. (2010) Activation and deactivation of DNAzyme and antisense function with light for the photochemical regulation of gene expression in mammalian cells. *J. Am. Chem. Soc. 132*, 6183−6193.
(63) Rivory, L., Tucker, C., King, A., Lai, A., Goodchild, A., Witherington, C., Gozar, M. M., and Birkett, D. J. (2006) The DNAzymes Rs6, Dz13, and DzF have potent biologic effects independent of catalytic activity. *Oligonucleotides 16*, 297−312.
(64) Martick, M., Horan, L. H., Noller, H. F., and Scott, W. G. (2008) A discontinuous hammerhead ribozyme embedded in a mammalian messenger RNA. *Nature 454*, 899−902.
(65) Kwok, T., Heinrich, J., Jung-Shiu, J., Meier, M. G., Mathur, S., and Moelling, K. (2009) Reduction of gene expression by a hairpin-loop structured oligodeoxynucleotide: Alternative to siRNA and antisense. *Biochim. Biophys. Acta 1790*, 1170−1178.
(66) Lin, Y., Dent, S. Y., Wilson, J. H., Wells, R. D., and Napierala, M. (2010) R loops stimulate genetic instability of CTG.CAG repeats. *Proc. Natl. Acad. Sci. U.S.A. 107*, 692−697.
(67) Wu, H., Lima, W. F., Zhang, H., Fan, A., Sun, H., and Crooke, S. T. (2004) Determination of the role of the human RNase H1 in the pharmacology of DNA-like antisense drugs. *J. Biol. Chem. 279*, 17181−17189.
(68) Kawada, M., Inoue, H., Masuda, T., and Ikeda, D. (2006) Insulin-like growth factor I secreted from prostate stromal cells mediates tumor-stromal cell interactions of prostate cancer. *Cancer Res. 66*, 4419−4425.
(69) Kawada, M., Inoue, H., Ohba, S., Masuda, T., Momose, I., and Ikeda, D. (2010) Leucinostatin A inhibits prostate cancer growth through reduction of insulin-like growth factor-I expression in prostate stromal cells. *Int. J. Cancer 126*, 810−818.
(70) Miyamoto, S., Nakamura, M., Shitara, K., Nakamura, K., Ohki, Y., Ishii, G., Goya, M., Kodama, K., Sangai, T., Maeda, H., Shi-Chuang, Z., Chiba, T., and Ochiai, A. (2005) Blockade of paracrine supply of insulin-like growth factors using neutralizing antibodies suppresses the liver metastasis of human colorectal cancers. *Clin. Cancer Res. 11*, 3494−3502.